TABLE 1 Comparison of the Proposed UWB Filter

Ref.	Circuit area (mm^2)	No. of notches/notch frequencies GHz)	No. of transmission zeros
[8]	295	1/5.8	2
[10]	604	3/5.2, 5.85, 8.0	1
[13]	435	3/5.2, 5.8, 8.0	2
[14]	263	2/6.55, 8.62	2
[17]	613	2/3.6, 5.9, 8.0	1
This work	203	3/5.4, 5.8, 8.2	2

proposed UWB filter with other recently reported notch band UWB filters in Table 1 show the proposed filter is substantially smaller.

6. CONCLUSION

A novel planar UWB bandpass filter structure that employs wave cancellation technique is presented. The design incorporates triple notch bands within the filter's passband that can be tuned individually. The filter was fabricated and characterized to verify the design. Notch bands at 5.4, 5.8, and 8.3 GHz had a corresponding 10 dB fractional bandwidth of 9%, 4.4%, and 9.4%, respectively. The proposed structure allows the notch bands to be tuned over a greater frequency range than other reported notch band UWB filters, which makes the proposed technique more flexible and versatile for various applications. The filter has characteristics of low-loss, quasi-elliptic function sharp 3-dB roll-off, and a wide out of band rejection. The size of the proposed filter is significantly smaller than previously published notched band UWB filters.

REFERENCES

1. Revision of Part 15 of the Commission's Rules Regarding Ultra-Wideband Transmission System, ET-Docket 98–153, First Note and Order Federal Communication Commission, 2002.
2. L. Zhu, S. Sun, and W. Menzel, "Ultra-wideband (UWB) bandpass filter using multiple-mode resonator", IEEE Microwave Wireless Compon Lett 15 (2005), 796–798.
3. S.B. Cohn, "Parallel coupled transmission∼Line∼resonator filters", IRE Trans Lett 3 (1955), 29–38.
4. S. Oh, J. Song, and J. Lee, "UWB Bandpass Filter Based on Ring Resonator", Microwave Opt Technol Lett 55 (2013), 2047–2051.
5. D. Jhariya, A.R. Azad, A. Mohan, and M. Sinha, "A compact modified U-shaped UWB bandpass filter," Microwave Opt Technol Lett 57 (2015), 2172–2175.
6. H. Shaman and J.S. Hong, "Ultra-wideband (UWB) bandpass filter with embedded band notch structures," IEEE Microwave Wireless Compon Lett 17 (2007), 193–195.
7. M. Amin Honarvar and R.A. Sadeghzadeh, "Design of coplanar waveguide ultrawideband bandpass filter using stub-loaded resonator with notched band," Microwave Opt Technol Lett 54 (2012), 2056–2061.
8. X.Y. Zhang, Y.-W. Zhang, and Q. Xue, "Compact band-notched UWB filter using parallel resonators with a dielectric overlay," IEEE Microwave Wireless Compon Lett 23 (2013), 252–254.
9. M. Mirzaee and B.S. Virdee, "UWB bandpass filter with notch-band based on transversal signal-interaction concepts," Electron Lett 49 (2013), 399–401.
10. K. Song, T. Pan, and Q. Xue, "Asymmetric dual-line coupling strip for multiple notched bands: Theory and implementation," SciVerse Sci Direct Microelectron J 43 (2012), 416–422.
11. S.J. Borhani, M.A. Honarvar, and B.S. Virdee, "High selectivity UWB bandpass filter with a wide notched-band," Microwave Opt Technol Lett 57 (2015), 634–639.
12. F. Wei, W.T. Li, and X.W. Shi, "Compact UWB bandpass filter with triple-notched bands using triple-mode stepped impedance resonator," IEEE Microwave Wireless Compon Lett 22 (2012), 512–514.
13. J. Wang, J. Zhao, and J. -L. Li, "Compact UWB bandpass filter with triple notched bands using parallel U-shaped defected microstrip structure," Electron Lett 50 (2014), 89–91.
14. M. Nosrati and M. Daneshmand, "Compact microstrip ultra-wideband double/single notch-band band-pass filter based on wave's cancellation theory," IET Microwave Antennas Propag 6 (2012), 862–868.
15. M. Nosrati and M. Daneshmand, "Developing single-layer ultra-wideband band-pass filter with multiple (triple and quadruple) notches," IET Microwave Antennas Propag 7 (2013), 612–620.
16. J.S. Hong, "Microstrip Filters for RF/Microwave Applications," 2nd ed., K. Chang (Ed.), John Wiley & Sons, Inc., New Jersey. Hoboken, 2011.
17. F. Wei, Z.D. Wang, F. Yang, and X.W. Shi, "Compact UWB BPF with triple-notched bands based on stub loaded resonator," Electron Lett 49 (2013), 124–126.

TWO-ARM ARCHIMEDEAN SPIRAL ANTENNA FED BY BROADBAND DOUBLE SIDED PARALLEL STRIP LINE

Seongwon Oh[1] and Chihyung Ahn[2]
[1] Agency for Defense Development, Jinhae-Gu, Changwon 51698, Korea; Corresponding author: osw123@add.re.kr
[2] Korea Railroad Research Institute, Uiwang 16105, Korea

Received 15 December 2015

ABSTRACT: *This paper is intended to introduce a two-arm Archimedean spiral antenna fed by a novel feed structure based on DSPSL (Double Sided Parallel Strip Line). A DSPSL provides an ease perpendicular matching network and an impedance transition between input impedance of a spiral antenna and system's impedance of 50 Ω in broadband frequency range. Measured and simulated VSWR and radiation pattern results show a good performance over ultra-wide band from 2 to 20 GHz.* © 2016 Wiley Periodicals, Inc. Microwave Opt Technol Lett 58:1879–1883, 2016; View this article online at wileyonlinelibrary.com. DOI 10.1002/mop.29931

Key words: *spiral antenna; double sided parallel strip line; balun*

1. INTRODUCTION

An Archimedean spiral antenna designed by Kaiser in 1960 has been widely used in communication and other systems for its wideband bandwidth and radiation characteristics [1]. Since a spiral antenna is a balanced structure, its feed structure needs a balun to transform an unbalanced line into a balanced line. Although the spiral antenna itself is a very wideband component, the whole antenna performance could be degraded because of the limits of a balun [2] To overcome the degradation, some innovative feed designs were applied to spiral antennas including a microstrip-coplanar stripline feed [2], a 3-arm spiral antenna with a planar CPW feed [3], a stripline-based inward feed in multilayer substrates [4,5] and a parallel-plane perpendicular current feed [6]. These designs show a good performance, but their structures are two-dimensional, so the feed structures parallel to the plane of the spiral make unwanted coupling between the feed lines and the spiral antenna, and the whole antenna footprint become bigger. These characteristics may not be desirable for some applications using array structures or requiring less coupling from the feed network.

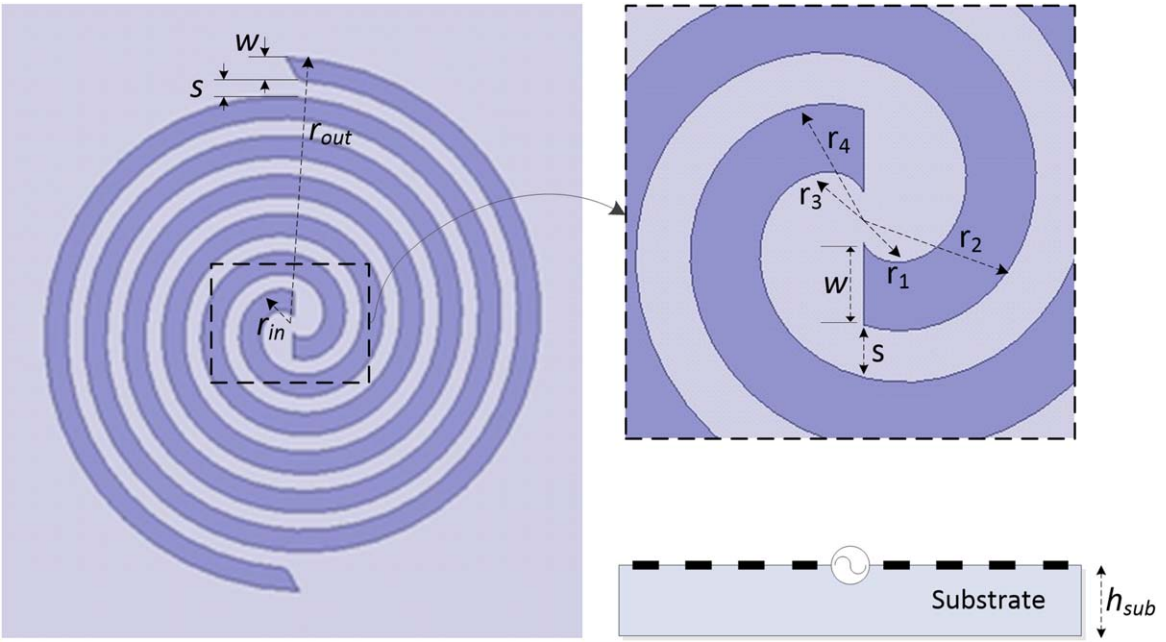

Figure 1 Geometry of the two-arm Archimedean spiral antenna. [Color figure can be viewed in the online issue, which is available at wileyonlinelibrary.com]

For perpendicular feeding, a CPW-CPS balun [7] and a tapered coax balun [8] have been implemented, but their structures are too complicated and difficult to manufacture or install. A tapered microstrip balun [9], an alternative, is relatively easy to manufacture than the above. However, the DSPSL (Double Sided Parallel Strip Line) proposed by Wheeler in 1964 [10] could be a better choice than a tapered microstrip line because a DSPSL's impedance variation range is larger than a tapered strip line's in same dimension and it can be implemented at off-center feed points of an antenna. A DSPSL is made of two identical strip lines on the opposite sides of a dielectric substrate and has been widely used in RF circuits because of easy realization of lines with various characteristic impedance and simplicity in circuit structures of wideband transitions [11,12].

In this paper, an electromagnetic coupled balun formed microstrip line to Double Sided Parallel Strip Line (DSPSL) is proposed to feed a two-arm Archimedean spiral antenna. The proposed Archimedean antenna shows a good performance 2.5:1 VSWR over the measured frequency range (2–20 GHz) in a three-dimensional structure.

2. ANTENNA DESIGN

A two-arm Archimedean spiral antenna is presented to illustrate the DSPSL feed design. The highest and lowest operating frequencies of the spiral are determined by its inner and outer diameter, respectively.

Figure 1 shows the antenna geometry with inner radius $r_{in}(r_1=r_3)=0.67$ mm, outer radius $r_{out}=22$ mm, arm width $w = 2.23$ mm, and the space between two arms s = 1.4 mm using a RT/Duroid 5870 substrate with $\varepsilon_r=2.33$ and $h_{sub}=0.7847$ mm.

3. DSPSL TRANSITION DESIGN

Spiral antennas exhibit broadband behavior with high efficiency but it is difficult to feed these antennas without degrading the performances. Many designs mentioned previously show a good performance in planar structures. However, these planar feeding structures can create electromagnetic coupling between feeding lines and the arms of neighbor spiral antennas and finally require more space for the arrangement. The proposed DSPSL feeding design that connects the spiral antenna perpendicularly could eliminate these unwanted coupling in a small footprint.

Figure 2 illustrates the geometry of the DSPSL feed for the Archimedean spiral antenna using the same substrate with the spiral antenna. Any type of microstrip spiral antennas can adopt DSPSL feeds. The major cross-sections and their electric field distributions at three different locations are shown in Figure 3. It is noticed that section A–A' generates almost horizontally distributed electric fields because of its thin substrate thickness and wide gap between two signal lines. In section B–B', the

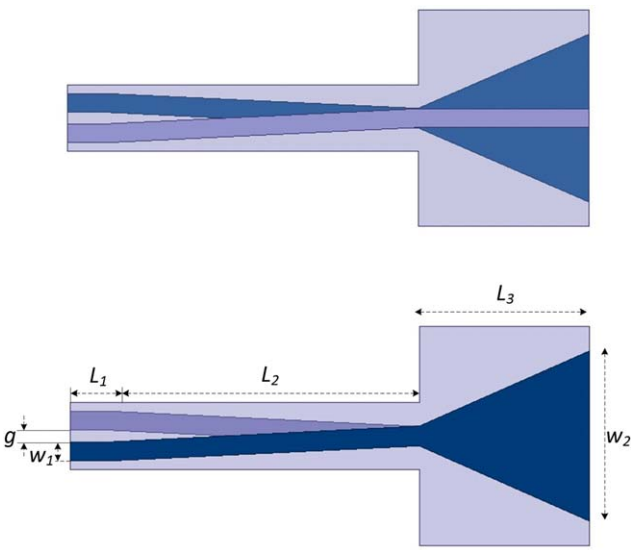

Figure 2 Geometry of the DSPSL feed structure (top and bottom plane) connected to the center of the spiral. [Color figure can be viewed in the online issue, which is available at wileyonlinelibrary.com]

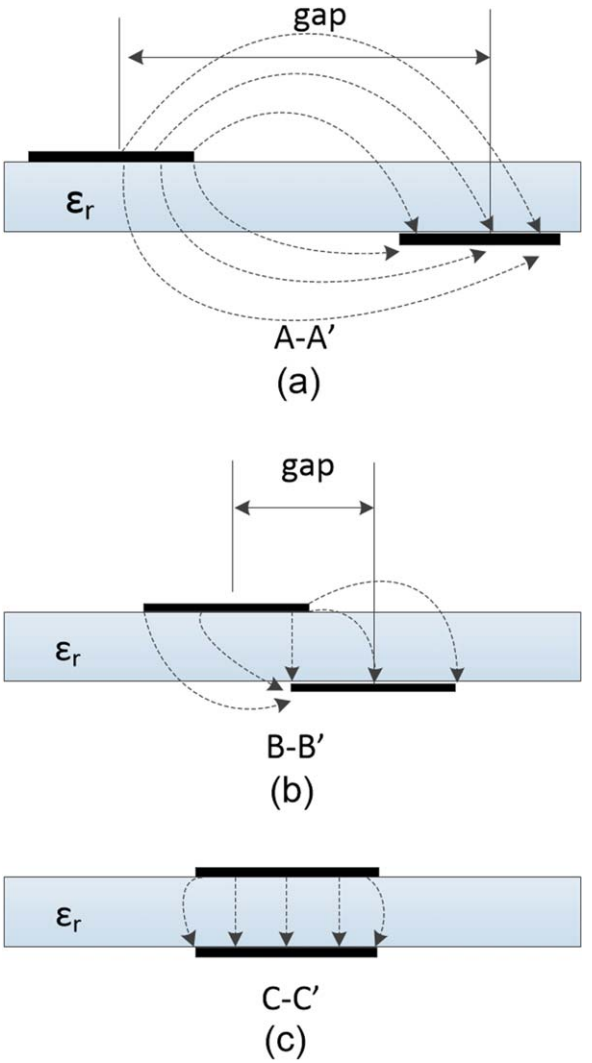

Figure 3 Cross sectional views of DSPSL transition and electric field distributions. [Color figure can be viewed in the online issue, which is available at wileyonlinelibrary.com]

horizontally distributed electric fields change to be vertically distributed. The changing fields have been almost converted to the vertical distribution in section C–C′. It is available to obtain impedance matching between the spiral antenna and the DSPSL by changing gap between two signal lines.

The characteristic impedance of section A–A′ can be analytically obtained by the equation below [10].

$$Z_{c\_wide}=377\varepsilon_r^{-\frac{1}{2}}\left(\frac{w}{h}+0.441+\left(\frac{\varepsilon_r+1}{2\pi\varepsilon_r}\right)\left(\ln\left(\frac{w}{h}+0.94\right)+1.451\right)+\frac{\varepsilon_r-1}{\varepsilon_r^2}(0.082)\right)^{-1}[\Omega]$$

where w and h are the strip width and substrate height, respectively. In this design, the DSPSL is synthesized by transforming the input impedance $Z_a=160\ \Omega$ of the spiral antenna into the system's impedance $Z_0=50\ \Omega$. Because each arm of the spiral antenna is attached to the microstrip line of DSPSL, DSPSL feed design is starting with the same width $w_1=2.23$ mm and the gap between the spiral arms $g = 1.35$ mm which are already determined. In this case, a tapered microstrip line cannot be used because the feed position of each arm is not symmetric and is

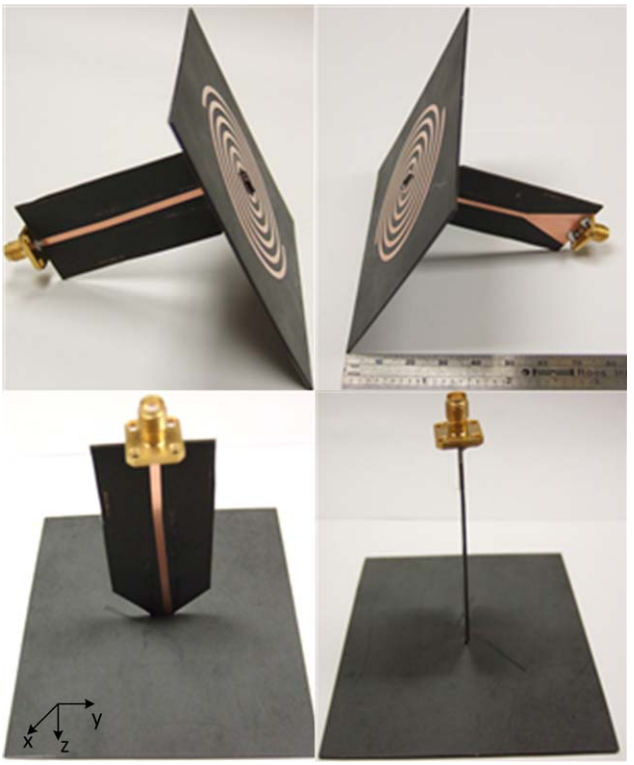

Figure 4 Fabricated spiral antenna with the DSPSL feed network. [Color figure can be viewed in the online issue, which is available at wileyonlinelibrary.com]

$(w + g)$ apart. DSPSL section length $L_1=5$ mm, the intermediate section $L_2=36$ mm, microstrip line section $L_3=20$ mm, and ground width $w_2=20$ mm. These dimensions are not optimized, so it can be adjusted to reduce the total length or to improve the performance of DSPSL. Also adapting a tapered ground and lines can enhance the total performance of the spiral antenna.

4. FABRICATION AND MEASUREMENTS

One of DSPSL's advantages is that DSPSL line width is wider than a microstrip line with the same characteristic impedance so it is easy to align DSPSL line to the spiral's feed points at high frequency band. The center of the spiral antenna is cut to a slot, and the arms are soldered onto the DSPSL lines as shown in Figure 4. The cutting and soldering works to the center of the

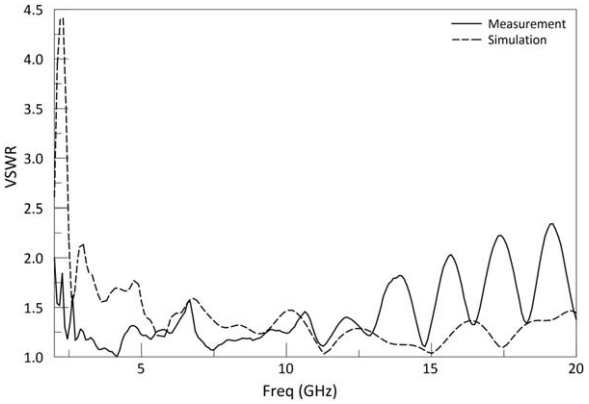

Figure 5 VSWR of the measured and simulated DSPSL-fed spiral antenna

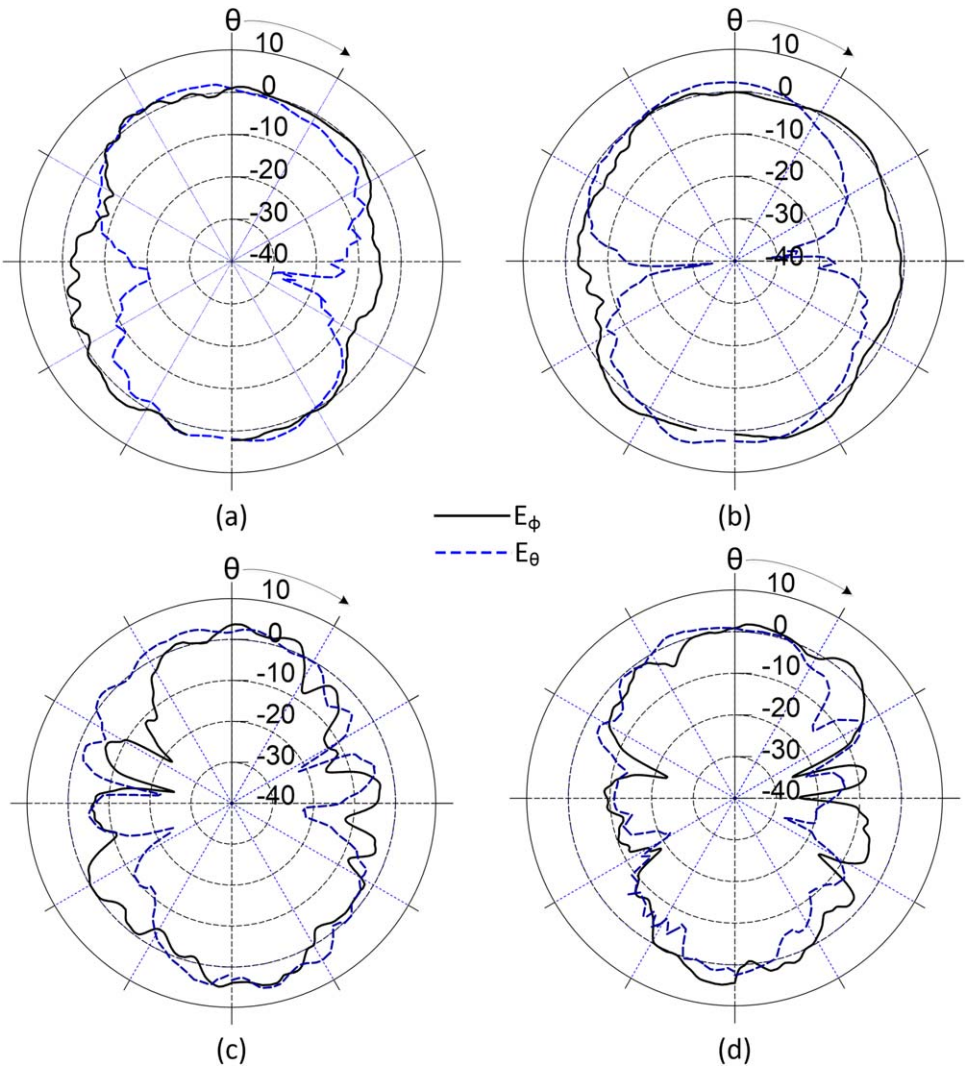

Figure 6 Measured radiation elevation patterns at 4 and 12 GHz (a) *xz plane* at 4 GHz, (b) *yz* plane at 4 GHz, (c) *xz plane at* 12 GHz, and (d) *yz* plane at 12 GHz. [Color figure can be viewed in the online issue, which is available at wileyonlinelibrary.com]

spiral and DSPSL feed were not exquisite, but the results show a good performance.

Figure 5 shows the VSWR of the measured and simulated spiral antenna. The VSWR remains below 2 over the whole range 2–20 GHz except 17.03–17.66 and 18.83–19.45 GHz, and the maximum VSWR is 2.37 at 19.19GHz.

Figure 6 shows the measured radiation patterns of the spiral antenna at 4 and 12 GHz. The radiation patterns of many designs that adopt a parallel feed to the antenna plane are asymmetric over 10 GHz because of their structural limits. However the proposed spiral antenna shows symmetric radiation patterns because the feed structure is perpendicular to the antenna plane and the geometry of the DSPSL feed do not affect the pattern from the spiral antenna.

5. CONCLUSION

A perpendicular off-center feed Archimedean spiral antenna based on DSPSL has been proposed. The DSPSL feed for the spiral antenna preserve the typical wideband operation and symmetric radiation behavior of the spiral antenna while making perpendicular feeding easily. The antenna showed a good measured result over 2 to 20GHz frequency range with 2:1 VSWR except 17.03–17.66 and 18.83–19.45 GHz and everywhere with 2.5:1 VSWR. The measured radiation patterns are symmetric over a whole frequency range. Exquisite cutting and assembling and a tapered ground plane could improve the performance of the spiral.

ACKNOWLEDGMENTS

The first author would like to thank the Agency of Defense Development, the Korea Railroad Research Institute and Texas A&M University for their technical supports.

REFERENCES

1. J.A. Kaiser, The Archimedean two-wire spiral antenna, IRE Trans Antennas Propag (1960), 312–323.
2. W.H. Tu, M.Y. Li, and K. Chang, Broadband microstrip-coplanar stripline-fed circularly polarized spiral antenna, IEEE Antennas and Propagation Society International Symposium, 2006, 3669–3672.
3. D.J. Müller and K. Sarabandi, Design and analysis of a 3-arm spiral antenna, IEEE Trans Antennas Propag 55 (2007), 258–266.
4. G.H. Huff and T.L. Roach, Stripline-based spiral antennas with integrated feed structure, impedance transformer, and dyson-style balun, IEEE Antennas and Propagation Society International Symposium, 2007, 2698–2701.
5. T.K. Chen and G.H. Huff, Stripline-fed Archimedean spiral antenna, IEEE Antennas Wireless Propag Lett 10 (2011), 346–349.

6. T.W. Eubanks and K. Chang, A compact parallel-plane perpendicular-current feed for a modified equiangular spiral antenna, IEEE Trans Antennas Propag 58 (2010), 2193–2202.
7. M.Y. Li, K. Tilley, J. McCleary, and K. Chang, Broadband coplanar waveguide-coplanar strip-fed spiral antenna, Electron Lett 31 (1995), 4–5.
8. P.C. Werntz and W.L. Stutzmann, Design, analysis and construction of an Archimedean spiral antenna and feed structure, Proc IEEE 1 (1989), 308–313.
9. N. Liu, P. Yang, and W. Wang, Design of a miniaturized ultra-wideband compound spiral antenna, IEEE International Conference on Microwave Technology & Computational Electromagnetics (ICMTCE), 2013, 255–258.
10. H. Wheeler, Transmission-line properties of parallel strips separated by a dielectric sheet, IEEE Trans Microwave Theory Tech 13 (1965), 172–185.
11. S.G. Kim and K. Chang, Ultrawide-band transitions and new microwave components using double-sided parallel-strip lines, IEEE Trans Microwave Theory Tech 52 (2004), 2148–2152.
12. J.-X. Chen, Double-sided parallel-strip line circuit analysis and applications to microwave component designs, Ph.D. thesis, City University of Hong Kong, 2008

RESONANCES OF ELECTROMAGNETIC OSCILLATIONS IN A SPHERICAL METAL NANOPARTICLE

B.A. Belyaev[1,2,3] and V.V. Tyurnev[1,2]
[1] Kirensky Institute of Physics, Siberian Branch, Russian Academy of Sciences, Krasnoyarsk, Russia; Corresponding author: belyaev@iph.krasn.ru
[2] Institute of Engineering Physics and Radio Electronics, Siberian Federal University, Krasnoyarsk, Russia
[3] Reshetnev Siberian State Aerospace University, Krasnoyarsk, Russia

Received 24 December 2015

ABSTRACT: *Electrodynamic analysis of plasma oscillations in a spherical metal nanoparticle is performed. It is shown that typical reduction in the frequency and quality factor of the resonances with increasing nanoparticle radius fades if the mode number grows. Depending on the particle radius, the resonant enhancement of the electric field might considerably either increase or decrease with increasing mode number.* © 2016 Wiley Periodicals, Inc. Microwave Opt Technol Lett 58:1883–1886, 2016; View this article online at wileyonlinelibrary.com. DOI 10.1002/mop.29930

Key words: *plasmonics; scattering; particles; resonators; resonant modes*

1. INTRODUCTION

It is well known that metal nanoparticles exhibit resonant properties under the impact of electromagnetic fields in the optical frequency range [1–3]. This phenomenon was discovered and explained as long ago as the beginning of the last century [4,5]. However, it is only in recent years the number of theoretical and experimental works on the optical properties of the metal nanoparticles begins to increase because of the development of nanotechnologies, and above all, the appearance of new problems in photonics and nanoelectronics. Resonances in metal nanoparticles are related to the oscillations of conduction electrons [6]. Their frequencies are considerably lower than the plasma frequency, ω^{p}, in continuous medium. Besides, the unloaded quality factor is sufficiently large for application. We note that the resonances occur due to both the skin depth in metals at optical frequencies and electron mean free path are much greater than the sizes of the articles.

Metal nanoparticles are widely used in biomedicine [7] and various biosensors are built using these [8]. These nanoparticles are also used for enhancing the effect of Raman scattering [9] and for the enhancement of fluorescence [10]. The possibility of applying these nanoparticles to the building of microwaveguides for the optical band is currently being investigated [11,12]. These microwaveguides represent chains of identical interacting nanoparticles, which can be considered as resonators, such that the chains have transparency windows for electromagnetic oscillations in the range of the resonant frequencies. We note that the wavelength of the propagating electromagnetic waves in the microwaveguides is much greater than the cross-sectional size of the nanoparticles of which they are formed. It is important to note also that analogous approaches are used in the design of waveguides based on interacting oscillating circuits [13] and microstrip resonators [14], which showed themselves to good advantage in the high and super-high frequency ranges.

In essence, such waveguides are passband filters of a high order whose bandwidth is proportional to the interaction of the resonators [15]. The interaction strength is determined first by the spacing between the resonators and their quality factor. However, in a chain of interacting resonators, including a chain of spherical nanoparticles, forming a waveguide, the coupling between the structural elements may weaken considerably if the resonant frequencies of these elements are mismatched. Therefore, it is important to study the regularities of the size-dependent behavior of the key resonance characteristics of the spherical metal nanoparticles when they are in a high-frequency electric field.

In this letter, we study the behavior of resonant frequencies, the quality factors of the resonances, near-field patterns, the enhancement coefficients of the electric field, and the frequency dependences of the scattering cross-sections of electromagnetic waves. We investigate three lower oscillation modes, taking into account the fact that the spherical resonators may efficiently interact not only at the frequency of the first oscillation mode but also at the frequencies of higher modes.

2. INITIAL FORMULAS

Let a spherical metal nanoparticle of radius r_0 be situated in a medium with relative permittivity ε_2 (Fig. 1). The dielectric properties of the nanoparticle material are described using the complex permittivity, $\varepsilon_1(\omega)$, that takes into account both dielectric and ohmic loss.

We shall consider the oscillations in the nanoparticle under the impact of an incident plane wave, with the following components of the electric and magnetic field

$$\begin{aligned} E_x(z,t) &= E_0 \exp\left(ik_2 z - i\omega t\right), \\ H_y(z,t) &= H_0 \exp\left(ik_2 z - i\omega t\right), \end{aligned} \tag{1}$$

where $k_2=\omega\sqrt{\varepsilon_0\varepsilon_2\mu_0}$, $H_0=E_0/Z_2$, $Z_2=\sqrt{\mu_0/(\varepsilon_0\varepsilon_2)}$, and ε_0 and μ_0 are the absolute permittivity and permeability of free space, respectively.

Using the general solution to this electrodynamic problem [16], we write the amplitudes of the nonzero components of the electric field of the scattered wave using a spherical coordinate system, for the convenience of further analysis, in the following form